

Chloride intracellular channel protein 2: prognostic marker and correlation with PD-1/PD-L1 in breast cancer

Tao Xu^{1,2,*}, Zhi Wang^{2,*}, Menglu Dong¹, Di Wu², Shujie Liao², Xingrui Li¹

¹Department of Thyroid and Breast Surgery, Tongji Hospital, Tongji Medical College of HUST, Wuhan 430030, Hubei, People's Republic of China

²Department of Obstetrics and Gynecology, Cancer Biology Research Center, Tongji Hospital, Tongji Medical College of HUST, Wuhan 430030, Hubei, People's Republic of China

*Co-first authors

Correspondence to: Xingrui Li, Shujie Liao; **email:** lixingrui@tjh.tjmu.edu.cn, sjliao@tjh.tjmu.edu.cn

Keywords: CLIC2, breast cancer, prognosis, PD-1/PD-L1, immune infiltration

Received: March 18, 2020

Accepted: June 29, 2020

Published: September 11, 2020

Copyright: Xu et al. This is an open-access article distributed under the terms of the Creative Commons Attribution License (CC BY 3.0), which permits unrestricted use, distribution, and reproduction in any medium, provided the original author and source are credited.

ABSTRACT

Immune checkpoint inhibition has emerged as an effective treatment for multiple solid tumors, including advanced-stage breast cancer (BC). During the past decade, the US Food and Drug Administration has approved a number of agents for immune checkpoint blockade (ICB). However, the limited data on monotherapy anti-tumor activity in BC underscores the need for robust predictive biomarker development. Here, we used weighted gene coexpression network analysis of genes differentially expressed between BC and normal tissue to identify genes coexpressed with programmed death-1 (PD-1) and its ligand (PD-L1). Tumor Immune Estimation Resource and Gene Expression Profiling Interaction Analysis were used to assess the relationship between gene expression and the abundance of tumor-infiltrating lymphocytes (TILs). We found that chloride intracellular channel protein 2 (CLIC2) was not only coexpressed with PD-1 and PD-L1, but its increased expression was associated with a favorable prognosis and enrichment of multiple TIL types, particularly CD8+ T cells. These results suggest that CLIC2 is a potentially useful biomarker for identifying BC patients who could benefit from ICB.

INTRODUCTION

Breast cancer (BC) is the most common cancer diagnosed in women and is a leading cause of cancer death [1]. Breast-conserving surgery or mastectomy, as well as radiation therapy may be used as part of a treatment plan. Chemotherapy, endocrine therapy, or targeted therapies may also be used, depending on cancer type and molecular test results [2, 3]. However, BC often does not respond to traditional treatment [4]; therefore, new treatment regimens are urgently needed, especially for the basal-like BC subtype. Clinical trials conducted with immune checkpoint blockade (ICB) hold promise for improving BC treatment [5]. Accelerated US Food and Drug Administration (FDA) approval of atezolizumab, in combination with nab-

paclitaxel for the treatment of metastatic triple-negative BC (TNBC), has stimulated enthusiasm for studying ICB agents [6, 7].

FDA has approved multiple ICB agents for melanoma and non-small cell lung carcinoma (NSCLC), and it has approved atezolizumab as a first line treatment for patients with metastatic TNBC [8]. In contrast to melanoma and NSCLC, however, ICB has not yet produced favorable benefits in BC. There are several possible reasons for this. (1) BC has not traditionally been considered immunogenic. Although not synonymous with the basal-like subtype, compared to melanoma or NSCLC, BC usually has a low number of tumor-infiltrating lymphocytes (TILs). (2) The low tumor mutational burden across BC subtypes reduces

ability to generate neoantigens that can stimulate antitumor immune responses [9]. (3) Robust predictive biomarkers for an ICB response have not yet been established. Given the relatively low response rate to ICB monotherapy, clinical trials combining ICB with radiotherapy, chemotherapy, or oncogene-targeted therapies (NCT02926196, NCT03036488) are needed. In addition, studies that investigate robust biomarkers for identifying BC patients who could benefit from ICB will be critical.

Previous studies have shown that at the time of diagnosis, high-level TILs correlate with better outcomes in patients with nonmetastatic, basal-like cancer treated with standard therapeutic regimens [10, 11]. This improvement also occurred in ERBB2-enriched BC that received the anti-HER2 antibody trastuzumab [12]. Overall, in basal-like and ERBB2-enriched BCs, a “hot” immune microenvironment, containing enriched TILs, is associated with a better prognosis, compared with a “cold” immune microenvironment, containing few TILs [13, 14]. TILs provide more significant outcomes in patients who receive ICB agents that activates intrinsic T cells to eliminate tumor cells than in patients who receive standard therapeutic regimens [15]. Here, TILs are not limited to T cells because, in the tumor microenvironment, T-cell activation is controlled by the interplay of ligand-receptor interactions between T cells, dendritic cells (DCs), and tumor-associated macrophages (TAMs) [16]. TILs respond to ICB, owing to complex feedback loops and intertwined immune system regulation mechanisms [2, 17]. Therefore, it is promising that biomarkers that infer the quantity of TILs could help with identifying patients who could benefit from ICB.

Numerous trials have found that PD-L1-positive tumors had a higher overall response rate to ICB agents in patients with melanoma, NSCLC, Merkel cell carcinoma, renal cell carcinoma, and colorectal cancer than those with PD-L1 negative tumors [18–20]. In October 2015, PD-L1 was approved by the FDA as a predictive biomarker for patients with NSCLC when receive pembrolizumab. Published phase 1 studies reported that patients with metastatic BC, who incorporated anti-PD-L1 antibody atezolizumab or avelumab, had a higher objective response rate (ORR) and a longer overall survival (OS) when TILs positively expressed PD-L1 [15, 21]. Additional studies have found that significant relationships between PD-L1 expression in TNBC cancer cells and better ORR could not be established when incorporating atezolizumab [22]. Additionally, the scoring systems used for determining PD-L1 expression varied in different trials, which challenged the convenience of using PD-L1 as a selection marker.

Based on these results, we concluded that genes coexpressed with programmed cell death (PD-1) and PD-L1 in cancer cells could be effective biomarkers for patients who receive ICB [23]. We found that high expression of chloride intracellular channel protein 2 (CLIC2) in BC was correlated with increased expression of PD-1 and PD-L1, and that a high CLIC2 mRNA level has been associated with a favorable prognosis. In addition, a positive relationship exists between CLIC2 expression and TIL quantities across all BC subtypes.

RESULTS

Hub gene expression clusters with PD-1 or PD-L1

Using the limma R Bioconductor software package, a total of 3,868 differentially expressed genes (DEGs) were identified between BC and normal tissue, of which 2,688 genes upregulated and 1,180 genes downregulated in BC (Supplementary Figure 1A and 1B). Based on DEGs, a weighted gene coexpression network analysis (WGCNA) was performed to locate the gene modules in which gene expression patterns were similar. Here, we used a scale-free network distribution for the connectivity genes when the soft-threshold β value equals 4 (Figure 1A and 1B). Next, several gene modules were identified using average linkage hierarchical clustering (Figure 1C). Eleven major gene modules were identified (Figure 1D), of which the Megreen module genes positively correlated with both PD-1 ($r = 0.98$, $p = 1 \times 10^{-200}$) (Figure 1E) and PD-L1 ($r = 0.71$, $p = 2.87 \times 10^{-64}$) (Figure 1F). To reduce the scope of genes that correlated with PD-1 or PD-L1, two hub gene clusters were obtained from the Megreen module. The cluster correlated with PD-1 contained 131 genes (Supplementary Figure 2A, Supplementary Table 1), whereas the cluster correlated with PD-L1 had 37 genes (Supplementary Figure 2B, Supplementary Table 1). Using the limma packages and WGCNA, we obtained hub gene clusters that co-expressed with PD-1 or PD-L1 in BC.

Hub gene clusters correlated with PD-1 and PD-L1 participated in immune response

To further explore PD-1 and PD-L1 correlation, we mapped hub gene clusters to biologic function and enrichment analysis. The top five overrepresented Gene Ontology (GO) categories correlated to PD-1 were immune response, signal transduction, inflammatory response, adaptive immune response, and tumor necrosis factor-mediated signaling pathway (Figure 2A, Table 1). The top five enrichment pathways identified were cytokine-cytokine receptor interaction, primary immunodeficiency, cell adhesion

molecules (CAMs), inflammatory bowel disease, and hematopoietic cell lineage (Figure 2B, Table 1). GO categories and enrichment analysis correlated to PD-L1, consistent with PD-1, demonstrating an association of immunity (Supplementary Figure 3A and 3B, Supplementary Table 2). The previous results demonstrate that genes correlated to PD-1 and PD-L1 primarily participate in key immune response pathways.

Identification of gene coexpression with PD-1 and PD-L1

We next tested the overlap between the two hub gene clusters, and a set of 34 genes were identified. Although most of these genes were highly expressed in BC than

in normal tissue, only two genes, chloride intracellular channel protein 2 (CLIC2) and syntaxin 11 (STX11) (Supplementary Figure 2C), were lowly expressed in BC tissue (Figure 3A and 3B). CLIC2 belongs to the CLIC family of conserved metazoan proteins; however, the nature and function of CLIC2 have yet to be elucidated. It was previously reported that CLIC2 is expressed predominantly in noncancerous tissues [24]. Our results are consistent with this finding. It has previously been reported that STX11 functions as a tumor suppressor gene in peripheral T-cell lymphomas [25]. Those genes that downregulated in cancer suggest that its full function may protect cells from tumorigenesis. It is important to note that when downregulated gene expression is corrected or with agents that mimic gene function, the cancer may increase PD-L1 and PD-1

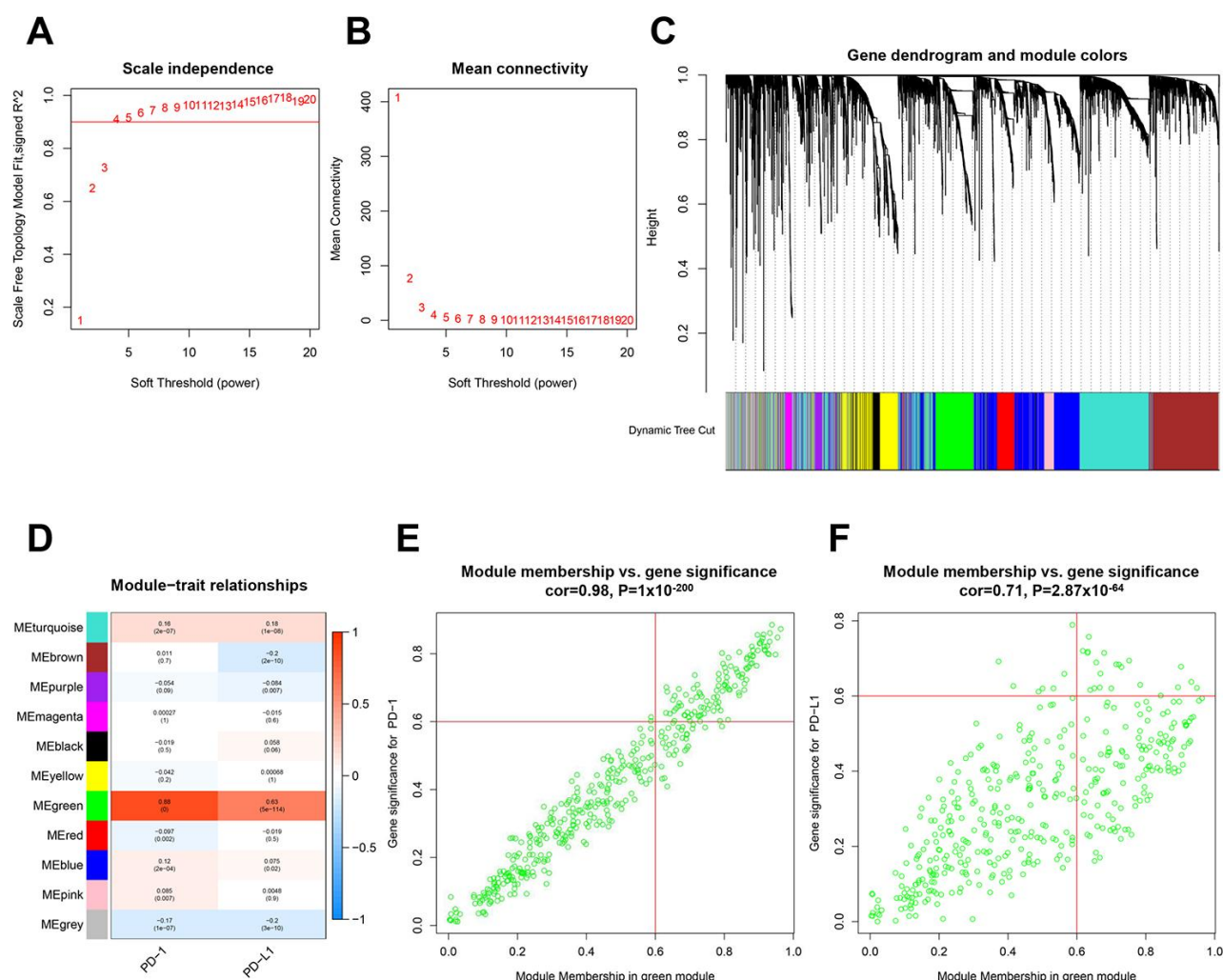
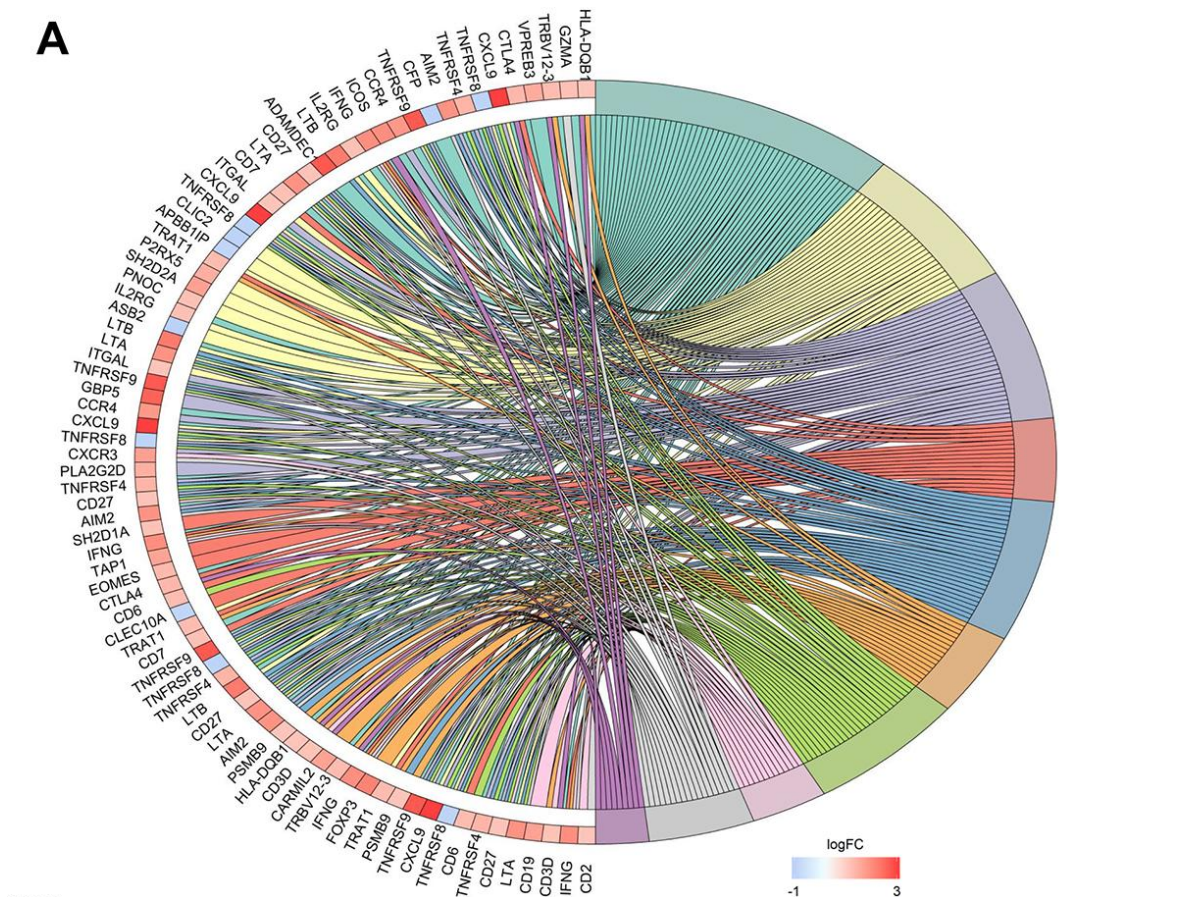


Figure 1. Identification of hub gene clusters that expressed with PD-1 or PD-L1 by WGCNA. (A) Plots visualize the scale-free topology fitting index. (B) The mean connection in different soft thresholds. (C) Branches of the hierarchical clustering dendrogram correspond to gene modules. (D) Heatmap of correlation between modules, eigengenes, and PD-1/PD-L1. Scatter plots visualize correlation between module membership in the Megreen module and gene signification for PD-1 (E) and PD-L1 (F). WGCNA, weighted gene co-expression network.

A



GO Terms



B

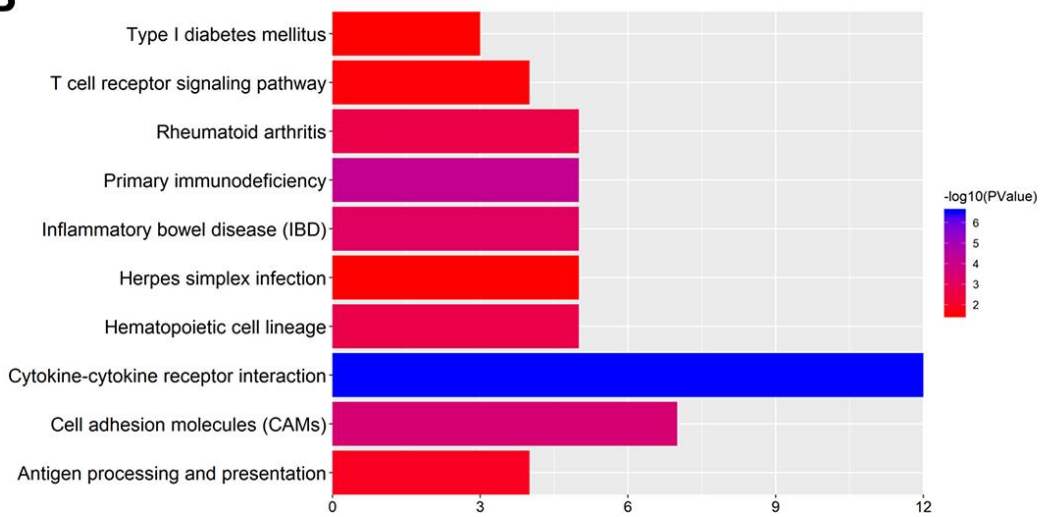


Figure 2. GO term and KEGG pathway enrichment analysis for the hub gene clusters. (A) Major GO terms in hub gene clusters correlated to PD-1. **(B)** Top-ranked KEGG pathways in hub gene clusters correlated to PD-1. GO, gene ontology; KEGG, Kyoto Encyclopedia of Genes and Genomes.

Table 1. GO and KEGG analysis of PD-1 co-expressing genes.

Term	Description	Count	P-value
GO:0006955	immune response	20	2.03E-14
GO:0007165	signal transduction	13	0.005114
GO:0006954	inflammatory response	11	6.85E-06
GO:0002250	adaptive immune response	9	3.09E-07
GO:0033209	tumor necrosis factor-mediated signaling pathway	8	9.46E-07
GO:0050852	T cell receptor signaling pathway	8	4.31E-06
GO:0032496	response to lipopolysaccharide	7	9.14E-05
GO:0007166	cell surface receptor signaling pathway	7	0.001403
GO:0006915	apoptotic process	7	0.040946
GO:0031295	T cell costimulation	6	2.54E-05
hsa04060	Cytokine-cytokine receptor interaction	12	2.99E-07
hsa05340	Primary immunodeficiency	5	6.42E-05
hsa04514	Cell adhesion molecules (CAMs)	7	0.000292
hsa05321	Inflammatory bowel disease (IBD)	5	0.000763
hsa04640	Hematopoietic cell lineage	5	0.002395
hsa05323	Rheumatoid arthritis	5	0.002498
hsa04612	Antigen processing and presentation	4	0.013188
hsa04660	T cell receptor signaling pathway	4	0.027223
hsa04940	Type I diabetes mellitus	3	0.030529
hsa05168	Herpes simplex infection	5	0.030930

expression, leading to increased curative effect of ICB. Therefore, CLIC2 and STX11 were selected for further study.

CLIC2 was associated with BC disease state and prognosis

To determine whether CLIC2 or STX11 was linked to BC clinical performance, Kaplan-Meier survival analysis was used on various BC subtypes. The Kaplan-Meier survival curves showed that higher CLIC2 mRNA levels were associated with longer OS (HR = 0.69 [0.55-0.86], $p = 0.00069$) (Figure 4A) and RFS (HR = 0.86 [0.77-0.96], $p = 0.0077$) (Figure 4B) in BC, whereas STX11 failed to demonstrate a significant relationship with OS (HR = 0.86 [0.69-1.06], $p = 0.16$) and RFS (HR = 0.92 [0.83-1.03], $p = 0.14$) (Supplementary Figure 4A and 4B). PrognoScan platform results showed that 5 out of 31 tests have an association between CLIC2 expression and favorable prognosis in BC, whereas other tests showed no significant correlations (Table 2). When BC cases were divided by clinical signatures (tumor size or disease stages), CLIC2 mRNA level in small tumor or early-stage cancer tissue was significantly higher than that in larger tumor or advanced-stage cancer tissue, respectively (Figure 4C and 4D). Notably, no difference in STX11 levels was observed in BC, regardless of size or stage (Supplementary Figure 4C and 4D). CLIC2 was more closely linked to clinical performance in BC than STX11. Thus, we chose CLIC2 for further study.

CLIC2 gene sets highly expressed cancer enriched in immune signal

To our knowledge, no study has specifically investigated the role of CLIC2 on immunity function and whether immunity response is based on CLIC2 mRNA levels. Therefore, we next performed a gene set enrichment analysis (GSEA) to determine whether high expression of CLIC2 BC samples was more active in immunity. A total of 1,053 BC tissue samples were divided into two groups. We demonstrated that the CLIC2 highly expressed gene set was enriched in cytokine-cytokine receptor interaction, CAMs, chemokine signaling pathway, hematopoietic cell lineage, JAK/STAT signaling pathway, and leukocyte transendothelial migration (Figure 5A–5F). These results indicate that immunity of CLIC2 highly expressed BC is more active compared with CLIC2 lowly expressed BC.

CLIC2 highly expressed BC was accompanied by increased TILs

Because increased TILs improve prognosis in BC patients receiving immunotherapy, we used the Tumor Immune Estimation Resource (TIMER) web server to access the correlation between CLIC2 expression and six TIL types. Figure 6 shows that CLIC2 expression has a positive correlation with infiltrating levels of six immune cell types, including B cells, CD4+ T cells, CD8+ T cells, neutrophils, TAMs, and

DCs, on total BC. Across all subtypes, CLIC2 expression positively correlated with all types of TIL enrichment in luminal cancer, whereas in basal-like cancer and HER-2 positive cancer, this relationship was also established between CLIC2 and all types of TIL enrichment, except for TAMs. This result, suggesting that CLIC2 highly expressed BC, was most likely

accompanied by increasing TILs. We also examined correlation between CLIC2 expression and TILs on other tumors decreased in CLIC2 (Supplementary Figure 5). Similar results were found, particularly in lung squamous cell carcinoma (LUSC) (Supplementary Figure 6A), colon adenocarcinoma (COAD) (Supplementary Figure 6B), stomach adenocarcinoma

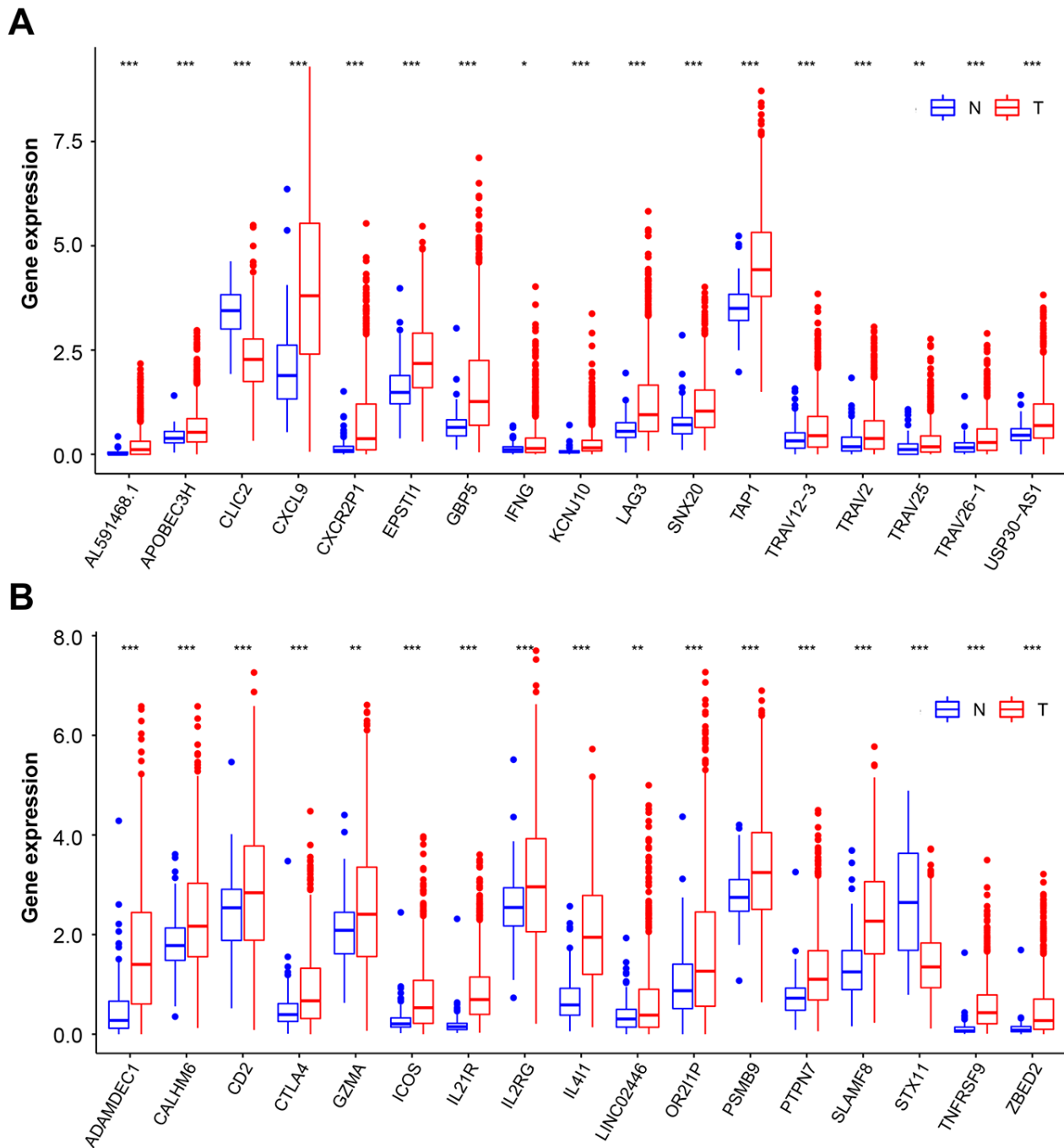


Figure 3. Overlapping genes expression on BC and normal tissue samples. (A and B) Box plot representation of 34 overlapping hub genes expression on normal tissue (blue box) and BC (red box) samples. The median, first quartile, and third quartile of expression on distribution are shown. BC, breast cancer. * $p < 0.05$, ** $p < 0.01$, *** $p < 0.001$.

(STAD) (Supplementary Figure 6C), and liver hepatocellular carcinoma (LIHC) (Supplementary Figure 6D). Our data showed that CLIC2 had a strong positive correlation with infiltrating levels of CD8+ T cells and DCs in these four cancer types.

CLIC2 highly expressed cancer was accompanied by increased TIL markers

To confirm that increased CLIC2 mRNA levels were associated with enriched TILs, we used the Gene Expression Profiling Interaction Analysis (GEPIA2) database. Consistent with TIMER results, the GEPIA2 data showed that CLIC2 mRNA levels were positively related to the abundance of multiple immune cells, including CD8+ T cells, B cells, TAMs, neutrophils,

and DCs (Figure 7A–7E). The lymphocyte-specific immune (LYM) metagene signature provided useful information for BC prognosis as well as immune phenotype [26]. We then tested whether CLIC2 mRNA levels correlate with LYM metagene signature. Figure 7F shows that CLIC2 strongly correlated with favorable LYM metagene signature. Previous GEPIA2 results support the conclusion that high CLIC2 mRNA levels in BC implied severe lymphocyte infiltration.

Immunohistochemistry (IHC) analysis revealed correlation between CLIC2 expression and CD45+ cells

We next performed large-scale tissue microarray (TMA) analysis using IHC on 99 BC tissues. Supplementary

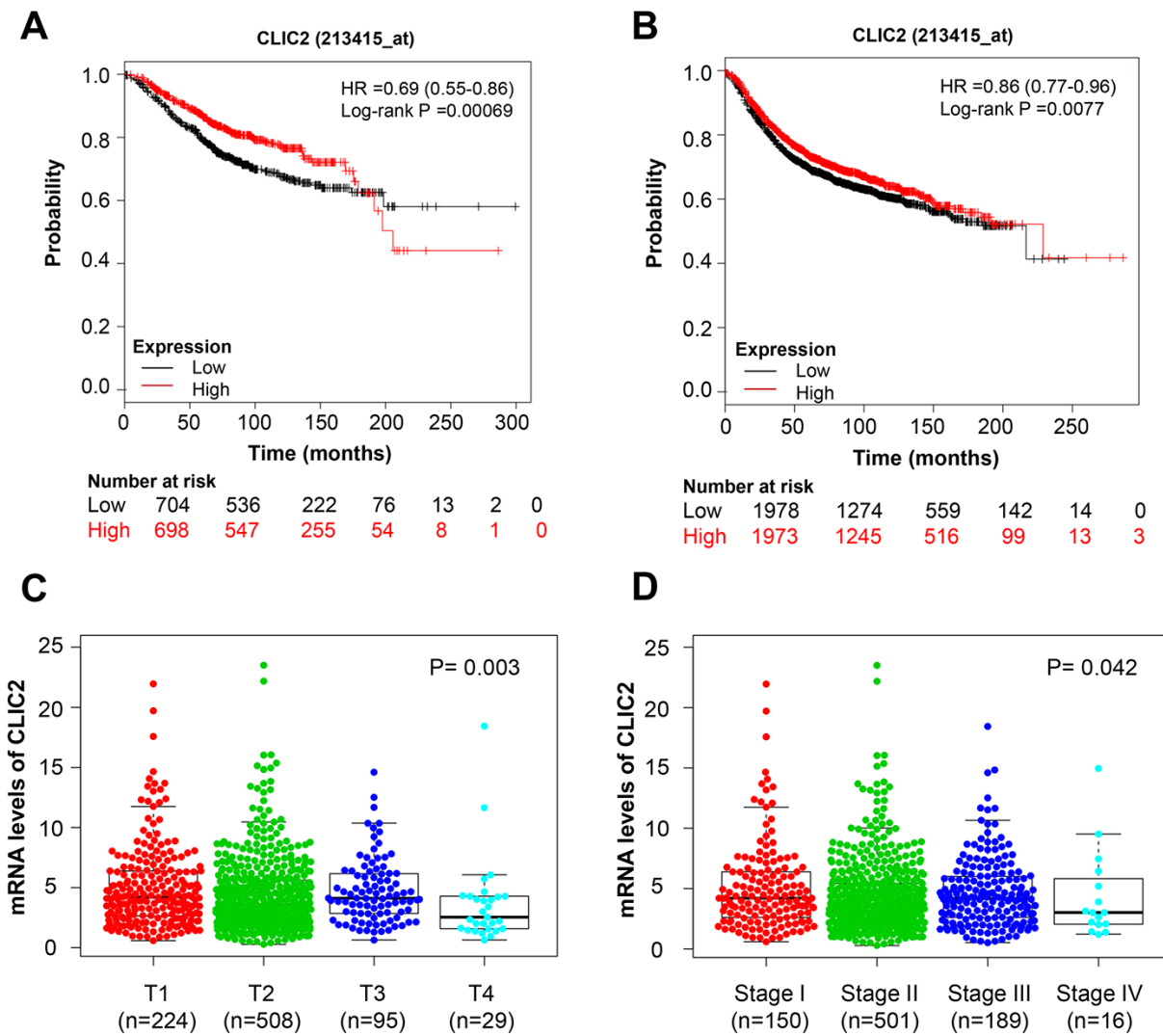


Figure 4. CLIC2 was associated with BC disease state and prognosis. Kaplan-Meier estimation of OS (A) and RFS (B) of TCGA BC patients grouped by CLIC2 expression. Gene CLIC2 expression profiles in BC with different tumor diameter (C) and in different stages (D). BC, breast cancer; OS, overall survival; PFS, progression-free survival.

Table 2. Survival analysis of CLIC2 mRNA in breast cancer patients (the Prognoscan database).

Dataset	Endpoint	Number	ln(HR-high / HR-low)	COX P-value	ln(HR)	HR [95% CI-low CI-up]
GSE1456	DSS	159	-1.14	0.01	-0.42	0.66 [0.48 - 0.91]
GSE3494	DSS	236	-1.02	0.02	-0.38	0.68 [0.50 - 0.95]
GSE1456	OS	159	-1.96	0.00	-0.42	0.65 [0.50 - 0.86]
GSE7378	DSS	54	-1.50	0.04	-1.49	0.22 [0.05 - 0.93]
GSE1456	RFS	159	-0.98	0.01	-0.36	0.70 [0.53 - 0.93]

Abbreviation: DSS, Disease Specific Survival; OS, Overall Survival; RFS, Relapse Free Survival; DFS, Disease Free Survival.

Table 3 shows the clinical characteristics of those patients. We examined and scored CLIC2 and CD45+ cell expression. Because CD45 is the common antigen that highly expressed in lymphocytes [27], we counted the anti-CD45 antibody- stained cells within stroma as TILs. Although tissue with no CLIC2 expression appeared to have rare TILs (Figure 8A), tissue with

increased CLIC2 expression had infiltrating lymphocytes (Figure 8B). Significant statistical analysis showed that fewer TILs were in the CLIC2 lowly expressed group than in the CLIC2 highly expressed group ($p < 0.0001$) or in the CLIC2 medium expressed group ($p < 0.01$) (Figure 8C), thus positive correlation between CLIC2 and TIL abundance.

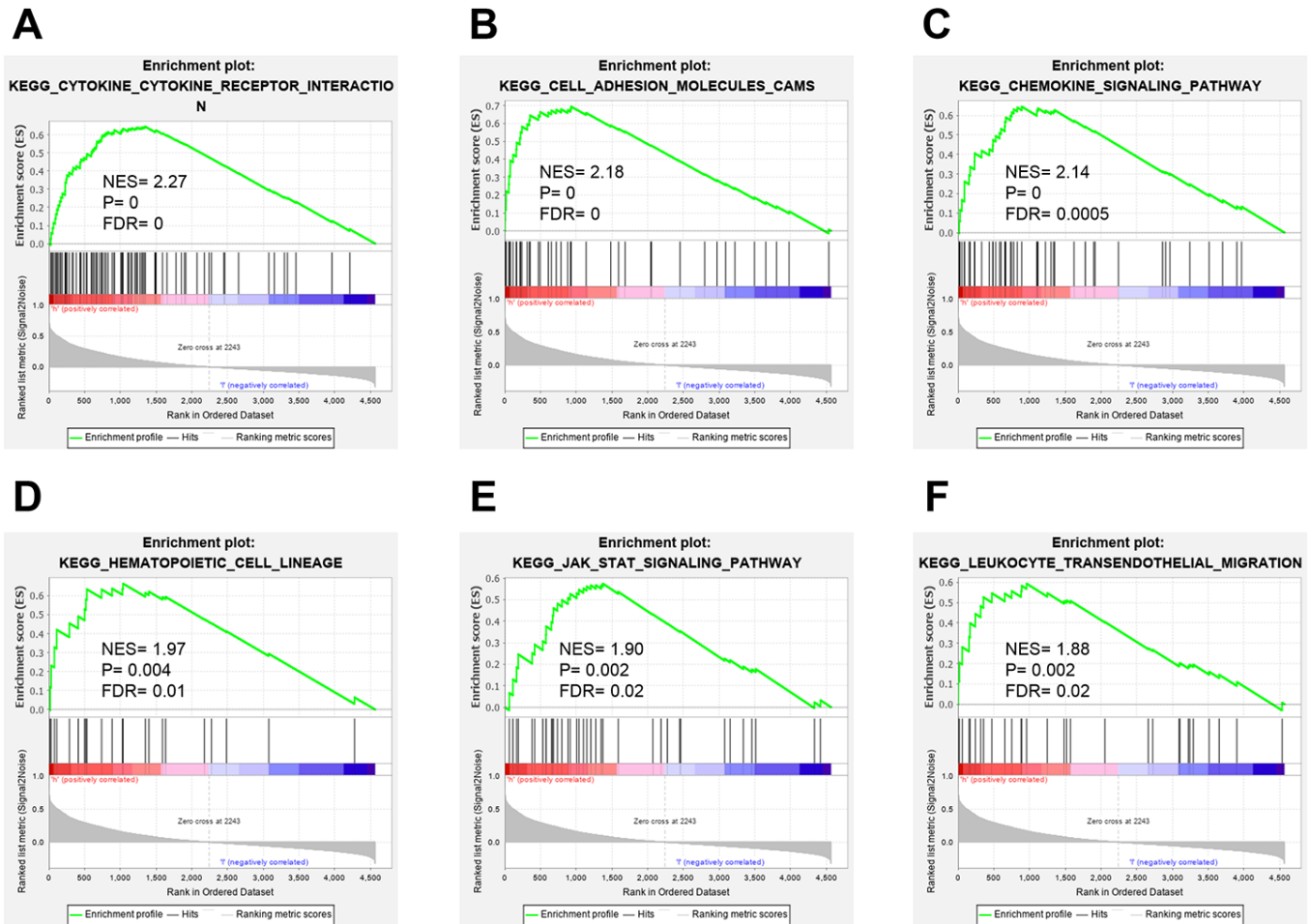


Figure 5. GSEA analysis of BC grouped by CLIC2 expression. GSEA was performed on RNA-Seq profiles of 1,053 breast cancer grouped by CLIC2 expression (high CLIC2 expression, $n = 526$; low CLIC2 expression, $n = 527$), and the top-ranked signatures were showing. (A) cytokine-cytokine receptor interaction; (B) cell adhesion molecules CAMs; (C) chemokine signaling pathway; (D) hematopoietic cell lineage; (E) JAK-STAT signaling pathway; (F) leukocyte transendothelial migration. GSEA, gene set enrichment analysis.

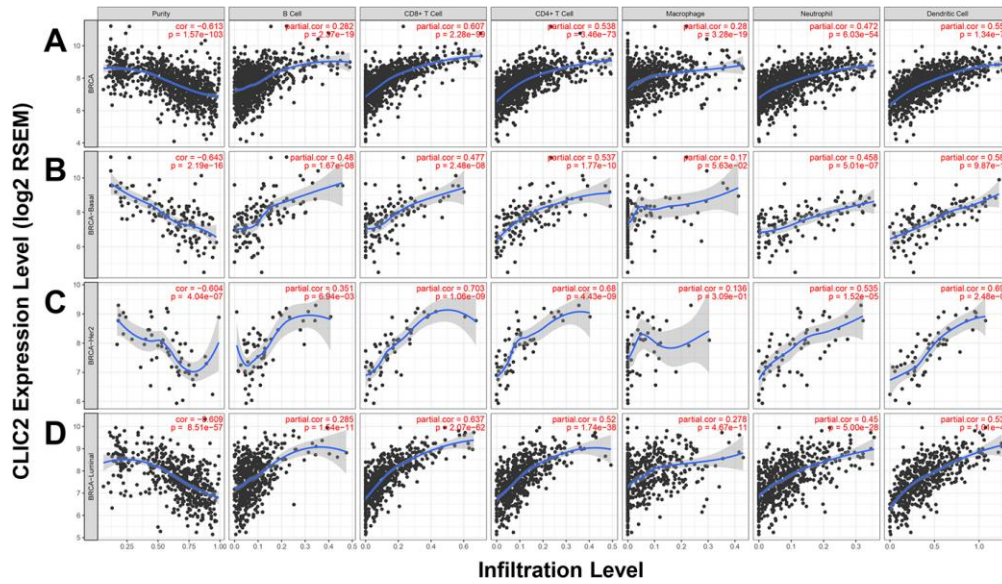


Figure 6. TIMER found CLIC2 highly expressed cancer was accompanied by increased TILs. (A) TIMER was performed to assess the correlation between CLIC2 expression and six types of TILs enrichment cross all subtypes of BC. Other than B cells and macrophages, CLIC2 expression has a strong positive correlation with CD8+ T cells, and moderate correlation with CD4+ T cells, neutrophils, and dendritic cells in BC. TIMER database analysis in (B) basal, (C) HER-2 and (D) luminal subtypes. TIMER, Tumor Immune Estimation Resource; TILs, tumor infiltration lymphocytes.

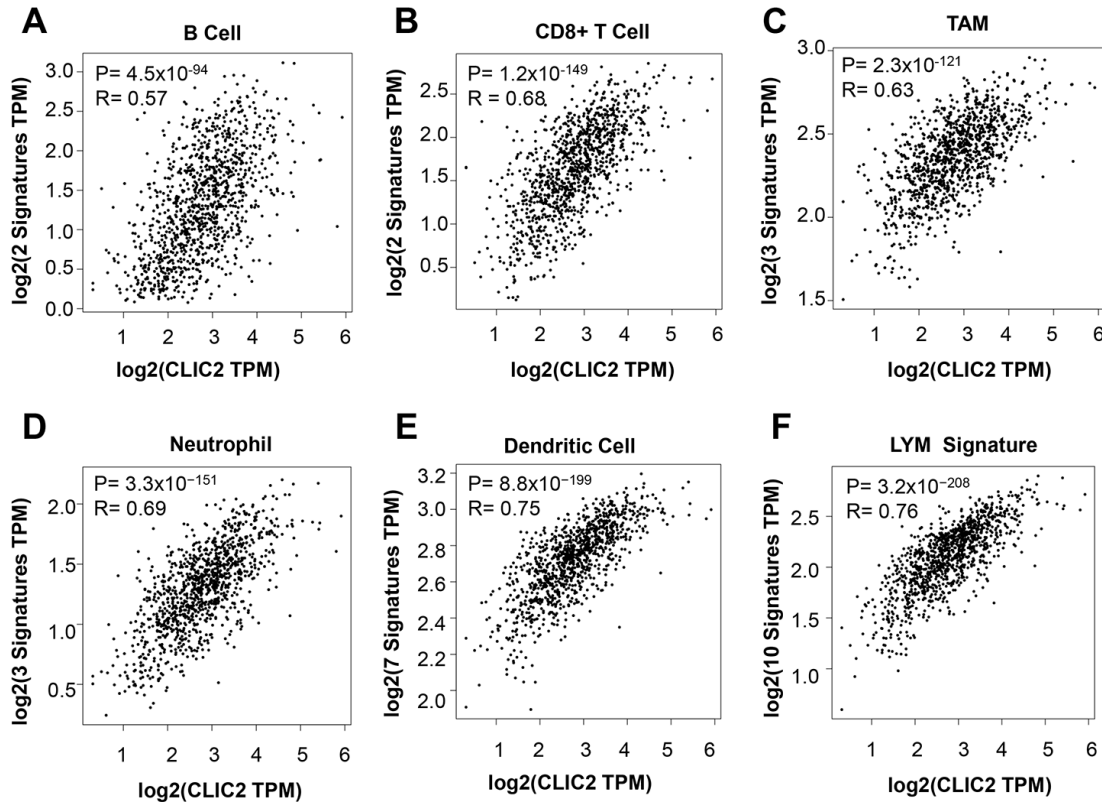


Figure 7. GEPIA2 found that CLIC2 highly expressed cancer was accompanied by increased markers of TILs. GEPIA2 was performed to assess the correlation between CLIC2 expression and markers of (A) CD8+ T cell, (B) B cell, (C) TAM, (D) neutrophil and (E) DC, and (F) LYM metagene signature. TAM, tumor-associated macrophage; DC, dendritic cell; LYM, lymphocyte-specific immune recruitment.

DISCUSSION

Here, we identified genes differentially expressed between BC and normal tissue, which coexpressed PD-1 and PD-L1. CLIC2 and STX11 were the only two genes that substantially decreased in BC. CLIC2 encodes a chloride intracellular channel protein (CLIC), whereas STX11 encodes a member of the syntaxin family. These two protein families have distinct functions. Studies on CLIC functions in tumors are more in-depth than those focused on syntaxin function. Given that CLIC2 has higher prognostic significance on BC patients than STX11, we believe further

examination of CLIC2 is needed. CLICs are highly conserved throughout metazoa, and currently six member genes have been reported [28, 29]. Among the CLICs, CLIC2 was the least investigated. Based on a previous study, CLIC2 could interact with and modulate the channel activity of RyR1 (ryanodine receptor 1) and RyR2 (ryanodine receptor 2) [30]. This indicates that CLIC2 may be a common modulator of Ca²⁺ release channels in cardiac and skeletal muscle. However, few studies have reported that CLIC2 had a physiological function in cancer or immunity. For the first time to our knowledge, our study found that CLIC2 in BC coexpressed with PD-1 and PD-L1. A recent study by

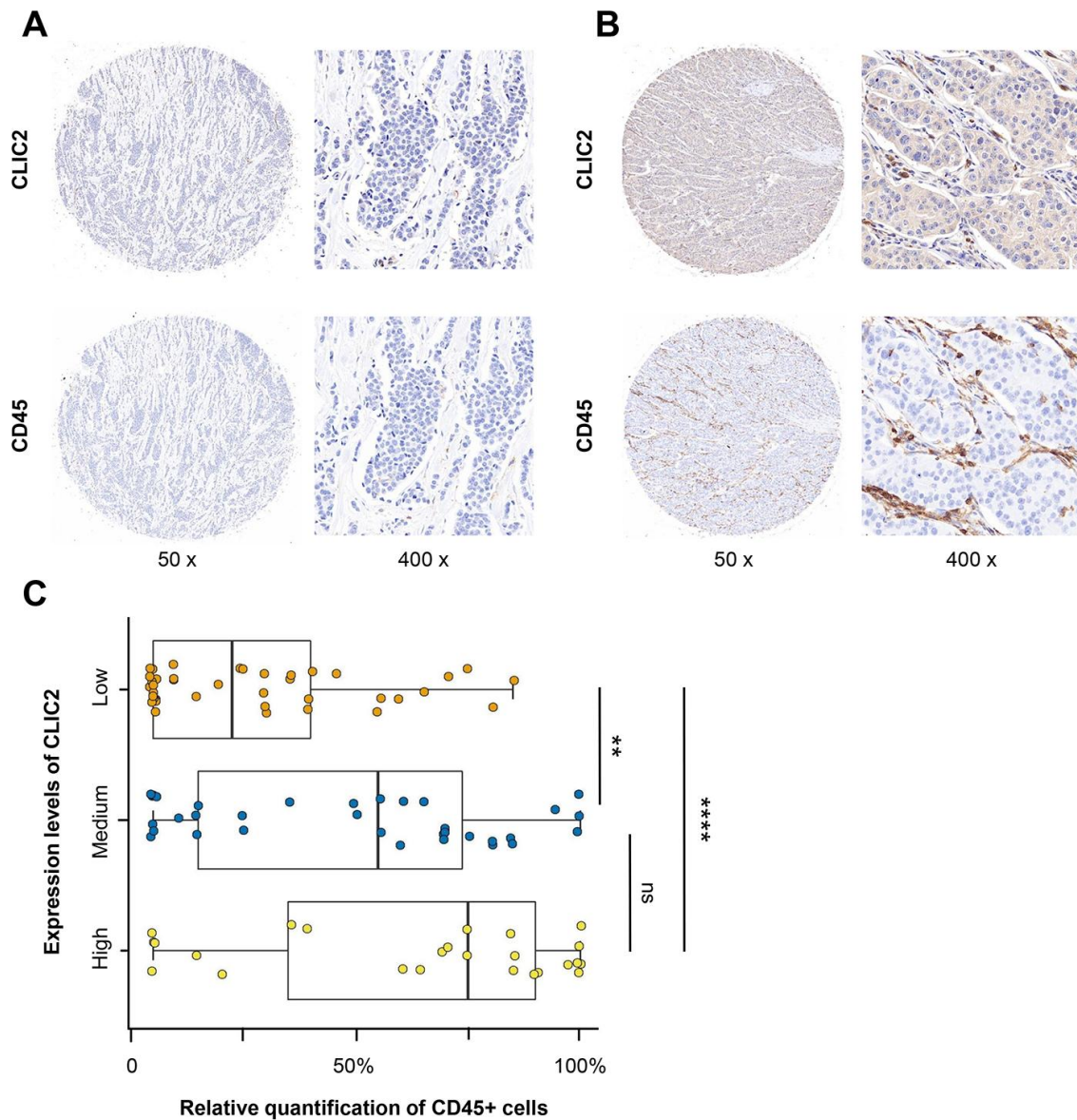


Figure 8. IHC analysis found that CD45+ cells were abundant in CLIC2 highly expressed tissue. (A) Low CLIC2 expression and low percentage of CD45+ cells. **(B)** High CLIC2 expression and high percentage of CD45+ cells. **(C)** Boxplot with scatter shows the different CD45+ cells percentage in tissue with different expression levels of CLIC2. ** p < 0.01, **** p < 0.0001.

Choy et al. used an unsupervised machine learning method to identify genes related to immune checkpoint proteins, including PD-1, PD-L1, and CTLA-4 [31]. According to their study, 13 genes, including CLIC2, were related to PD-1, and 26 other genes related to PD-L1. Our study provided additional evidence that CLIC2 expression is associated with PD-1. Although we found CLIC2 expression correlated with PD-L1, and Choy and colleagues failed to discover it, we attribute these findings to the different methodology that we used.

We found that high CLIC2 expression indicated a favorable prognosis in BC. However, CLIC2 mRNA expression in small tumor or early-stage cancer tissue was significantly higher than in larger tumor or advanced-stage cancer tissue, respectively. A previous study reported that CLIC2 mRNA expression at the early stage (stage IA) was significantly higher than at advanced stages (stage \geq IB) in hepatocellular carcinoma tissues [24]. In addition, the study reported that CLIC2 predominantly expressed in endothelial cells lining blood vessels, but not lymphatic vessels, in noncancerous tissues surrounding cancer masses, in which blood vessels might be in a state of loss-of-function of CLIC2. Ueno and colleagues also indicated that CLIC2 may be involved in the maintenance of tight junctions, and that cancer vasculature endothelial lacks CLIC2, allowing the hematogenous metastasis of cancer cells. Although this provided no direct evidence that high CLIC2 mRNA level was associated with enriched TILs, cancer blood vessels with CLIC2 high expression imply relative intact function of blood vessels in the initial stage cancer. Early-stage cancer is usually more intact on immune systems than advanced-stage cancer [32, 33]. However, we have not yet ascertained whether CLIC2 high expression caused TIL abundance or if it was a signal of enriched TILs. We hope this unanswered question motivates further studies. In addition to CLIC2, several other genes coexpressed with PD-1 and PD-L1 were found to be associated with the prognosis of BC patients. For example, Kaplan-Meier analysis data showed that GBP5, EPSTI1, IFNG, KCNJ10, LAG3, and SNX20 have positive correlation with RFS in BC patients, whereas TAP has reverse correlation with RFS (data not shown).

Our results demonstrate the association between CLIC2 mRNA level and TILs. The use of GSEA showed that expressed genes in BC, with increasing CLIC2 mRNA level, enriched an important immune-related pathway. The previous results support the hypothesis that CLIC2 plays an unknown role in the immune system. In addition to BC, CLIC2 significantly downexpressed in 13 other cancer types, including bladder urothelial carcinoma, cholangiocarcinoma, COAD, kidney carcinoma, including kidney chromophobe and kidney renal papillary cell carcinoma, LIHC, lung cancer,

including lung adenocarcinoma and LUSC, prostate adenocarcinoma, rectum adenocarcinoma, STAD, thyroid carcinoma, and uterine corpus endometrial carcinoma. The positive correlation between CLIC2 and abundant TILs were found on all of the previously stated carcinoma types, particularly LUSC, COAD, STAD, and LIHC. Those results indicated a common positive relationship between CLIC2 and TILs. Previously, it was reported that in LUSC, higher CD8+ TIL density was associated with longer disease-free survival [34]. Notably, pembrolizumab accompanying platinum-based chemotherapy has been approved as first-line treatment for patients with LUSC [35]. This indicated that, besides BC, higher CLIC2 expression may predict more abundant TILs and a more favorable prognosis in LUSC.

It is widely accepted that the presence of large quantities of TILs is a favorable prognostic marker in various solid tumors, including BC [11]. Clinical trial results have shown that TIL enrichment is a predictive response to the PD-1 antibody pembrolizumab, both in patients with HER2-positive BC (NCT02129556) or TNBC (KEYNOTE-086). Multifactorial markers incorporating PD-L1 expression, mutational load, intratumoral CD8+ T cells, and other variables may enhance predictive power contrast to individual tests for ICB agents [16]. Therefore, because CLIC2 coexpressed with PD-1 and PD-L1, and correlated with TIL quantities, we suggest that CLIC2 could be considered a member of predictive multifactorial markers to identify patients more likely to respond to PD-1 or PD-L1 inhibitors.

This study shows that CLIC2 coexpressed with PD-1 and PD-L1 in BC, and CLIC2 high expression was associated with a favorable prognosis and high quantities of TILs. These results suggest CLIC2 could be considered a potential biomarker to select BC patients who could derive benefit from ICB.

MATERIALS AND METHODS

Data collection

RNA-Seq filings along with paired clinical data of BC patients were retrieved from the publicly available TCGA (<https://www.cancer.gov/tcga>) database. In total, 1,053 tumor samples and 111 normal samples were collected. The RNA-seq filings were produced by Illumina HiSeq platform, and read counts were used to represent the gene expression level.

Identification of DEGs

The R version 2.6.2 [36] was used to process gene expression data. The limma package provided by

Bioconductor was used to screen the DEGs between tumor and normal samples [37]. Genes were considered as DEGs when (corrected $p < 0.05$ and $|\log_2\text{-fold-change}| > 1$).

Gene coexpression network construction and module detection

WGCNA was used to construct the coexpression network and detect modules as previously described [38, 39]. Pearson correlation matrices were generated for all DEGs. Using a power adjacency function, weighted adjacency matrix of connection strengths was transformed from coexpression similarities. Next, the adjacency matrix was transformed into a topological overlap matrix to survey relative gene interconnectedness and proximity. Here, the soft threshold β value equaled 4 when the co-expression network satisfied scale-free topology. Finally, gene modules were identified based on clustering according to the topology overlap.

Gene function and enrichment analysis

Hub genes were identified in the Megreen module when the Pearson's correlation coefficient > 0.6 and for PD-1 or PD-L1 when the Pearson's correlation coefficient > 0.6 . GO terms and the Kyoto Encyclopedia of Genes and Genomes (KEGG) pathway enrichment analysis were performed with the hub genes cluster by means of DAVID Bioinformatics Resources 6.8 (<https://david.ncifcrf.gov/>) [40]. A p value < 0.05 was considered statistically significant. To demonstrate common biological pathways shared by gene set in samples with CLIC2 high expression, 1,053 BC samples were divided into two groups based on whether CLIC2 expression was greater than the median value. GSEA software was used to examine the different pathways between these two groups, as previously described [41]. Enriched terms in the KEGG pathway, with normal $p < 0.05$ and false discovery rate value < 0.25 , were identified.

Kaplan-Meier and Prognosis survival analysis

The Kaplan-Meier plotter (<http://kmplot.com/>) [42] was used to analyze OS and progression-free survival on BC patients based on CLIC2 and STX11 expression. The patients were split by median value of gene expression. The Prognosis database, which is publicly accessible was examined to assess the relationship between gene expression and prognosis [43].

Correlated analysis with CLIC2 expression to TILs

TIMER (<https://cistrome.shinyapps.io/timer/>) database analysis was used to examine the correlation between CLIC2 expression and TILs [44]. GEPIA2

(<http://gepia.cancer-pku.cn/index.html>) database analysis was used to examine the correlation between CLIC2 expression and TIL markers [45]. The gene markers of TILs referred to a previous study [45, 46], including B cells, CD8+ T cells, TAMs, neutrophils, and DCs. The LYM metagene signature referred to previous study [26].

Immunohistochemical analysis and scoring

To examine the correlation between TILs and CLIC2 expression, IHC was performed on BC TMAs purchased from Avila (Cat No. DC-Bre11048) (Shanxi China) as previously described [47]. The anti-CD45 antibody (1:200; Catalog No. ab40763) and anti-CLIC2 antibody (1:200; Catalog No. ab175230) were purchased from Abcam. Semiquantitative scoring based on the staining intensity was used to evaluate CLIC2 expression (low, medium, and high) within the tumor cells. Anti-CD45 antibody-stained cells within the stroma were counted in the same location in which anti-CLIC2 antibody stained cells were quantified in another TMA. Scores were randomly examined by a second investigator, and an excellent intra-observer agreement was identified ($k = 0.9$).

Statistical analysis

The correlation of gene expression was accessed by Spearman's correlation coefficient. The correlations between clinical characteristics and CLIC2 expression were analyzed by a nonparametric test (the Wilcoxon test between two groups, and the Kruskal-Wallis test for three or more groups) [48]. In Kaplan-Meier survival analysis, p -value was calculated by multivariate Cox regression. The difference of TILs percentage of tissues on tissue microarrays was determined by using analysis of variance. A p -value less than 0.05 was considered significant.

AUTHOR CONTRIBUTIONS

XRL, SJL and TX conceived this project. ZW and TX performed the experiments. TX, MLD, and DW analyzed the data. ZW wrote the first manuscript. TX, XRL, and SJL reviewed and polished the manuscript. All authors read and approved the final manuscript for publication.

CONFLICTS OF INTEREST

The authors declare that there are no conflicts of interest.

FUNDING

This study was supported in part by the Wuhan Youth Cadre Project (2017zqnlxr01 and 2017zqnlxr02).

REFERENCES

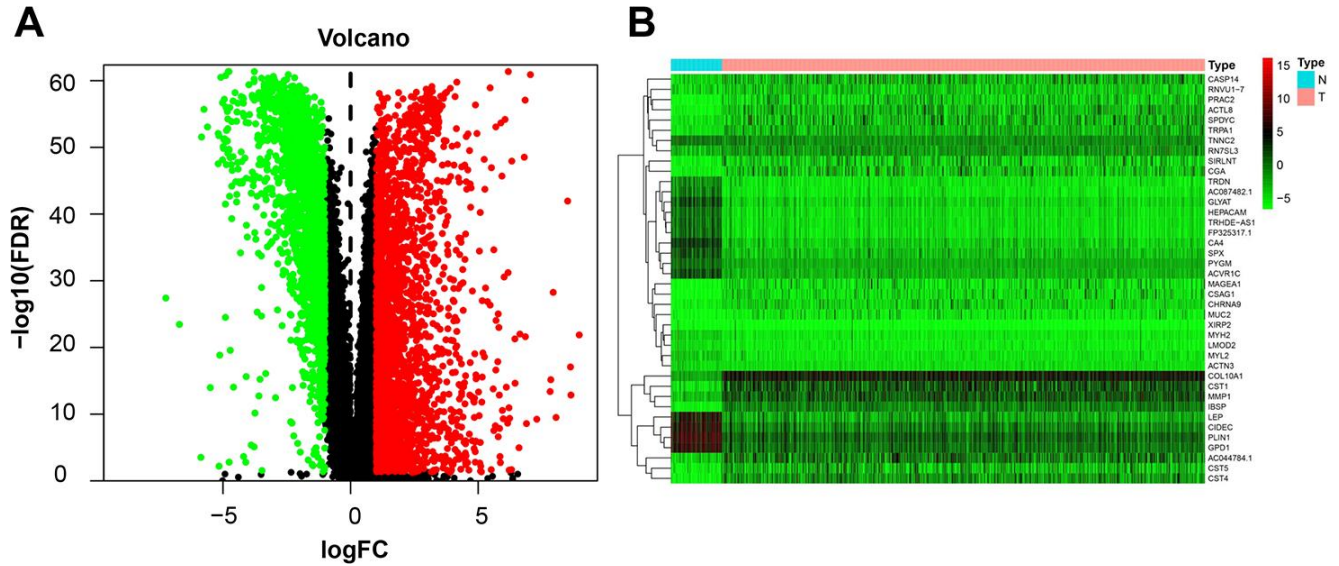
1. Bray F, Ferlay J, Soerjomataram I, Siegel RL, Torre LA, Jemal A. Global cancer statistics 2018: GLOBOCAN estimates of incidence and mortality worldwide for 36 cancers in 185 countries. *CA Cancer J Clin*. 2018; 68:394–424.
<https://doi.org/10.3322/caac.21492>
PMID:[30207593](https://pubmed.ncbi.nlm.nih.gov/30207593/)
2. Esteva FJ, Hubbard-Lucey VM, Tang J, Pusztai L. Immunotherapy and targeted therapy combinations in metastatic breast cancer. *Lancet Oncol*. 2019; 20:e175–86.
[https://doi.org/10.1016/S1470-2045\(19\)30026-9](https://doi.org/10.1016/S1470-2045(19)30026-9)
PMID:[30842061](https://pubmed.ncbi.nlm.nih.gov/30842061/)
3. Waks AG, Winer EP. Breast cancer treatment: a review. *JAMA*. 2019; 321:288–300.
<https://doi.org/10.1001/jama.2018.19323>
PMID:[30667505](https://pubmed.ncbi.nlm.nih.gov/30667505/)
4. Cancer Genome Atlas Network. Comprehensive molecular portraits of human breast tumours. *Nature*. 2012; 490:61–70.
<https://doi.org/10.1038/nature11412>
PMID:[23000897](https://pubmed.ncbi.nlm.nih.gov/23000897/)
5. Adams S, Gatti-Mays ME, Kalinsky K, Korde LA, Sharon E, Amiri-Kordestani L, Bear H, McArthur HL, Frank E, Perlmutter J, Page DB, Vincent B, Hayes JF, et al. Current landscape of immunotherapy in breast cancer: a review. *JAMA Oncol*. 2019; 5:1205–14.
<https://doi.org/10.1001/jamaoncol.2018.7147>
PMID:[30973611](https://pubmed.ncbi.nlm.nih.gov/30973611/)
6. Schmid P, Adams S, Rugo HS, Schneeweiss A, Barrios CH, Iwata H, Diéras V, Hegg R, Im SA, Shaw Wright G, Henschel V, Molinero L, Chui SY, et al, and IMpassion130 Trial Investigators. Atezolizumab and nab-paclitaxel in advanced triple-negative breast cancer. *N Engl J Med*. 2018; 379:2108–21.
<https://doi.org/10.1056/NEJMoa1809615>
PMID:[30345906](https://pubmed.ncbi.nlm.nih.gov/30345906/)
7. Schmid P, Rugo HS, Adams S, Schneeweiss A, Barrios CH, Iwata H, Diéras V, Henschel V, Molinero L, Chui SY, Maiya V, Husain A, Winer EP, et al, and IMpassion130 Investigators. Atezolizumab plus nab-paclitaxel as first-line treatment for unresectable, locally advanced or metastatic triple-negative breast cancer (IMpassion130): updated efficacy results from a randomised, double-blind, placebo-controlled, phase 3 trial. *Lancet Oncol*. 2020; 21:44–59.
[https://doi.org/10.1016/S1470-2045\(19\)30689-8](https://doi.org/10.1016/S1470-2045(19)30689-8)
PMID:[31786121](https://pubmed.ncbi.nlm.nih.gov/31786121/)
8. Ribas A, Wolchok JD. Cancer immunotherapy using checkpoint blockade. *Science*. 2018; 359:1350–55.
<https://doi.org/10.1126/science.aar4060>
PMID:[29567705](https://pubmed.ncbi.nlm.nih.gov/29567705/)
9. Lawrence MS, Stojanov P, Polak P, Kryukov GV, Cibulskis K, Sivachenko A, Carter SL, Stewart C, Mermel CH, Roberts SA, Kiezun A, Hammerman PS, McKenna A, et al. Mutational heterogeneity in cancer and the search for new cancer-associated genes. *Nature*. 2013; 499:214–18.
<https://doi.org/10.1038/nature12213>
PMID:[23770567](https://pubmed.ncbi.nlm.nih.gov/23770567/)
10. Loi S, Sirtaine N, Piette F, Salgado R, Viale G, Van Eenoo F, Rouas G, Francis P, Crown JP, Hitre E, de Azambuja E, Quinaux E, Di Leo A, et al. Prognostic and predictive value of tumor-infiltrating lymphocytes in a phase III randomized adjuvant breast cancer trial in node-positive breast cancer comparing the addition of docetaxel to doxorubicin with doxorubicin-based chemotherapy: BIG 02-98. *J Clin Oncol*. 2013; 31:860–67.
<https://doi.org/10.1200/JCO.2011.41.0902>
PMID:[23341518](https://pubmed.ncbi.nlm.nih.gov/23341518/)
11. Savas P, Salgado R, Denkert C, Sotiriou C, Darcy PK, Smyth MJ, Loi S. Clinical relevance of host immunity in breast cancer: from TILs to the clinic. *Nat Rev Clin Oncol*. 2016; 13:228–41.
<https://doi.org/10.1038/nrclinonc.2015.215>
PMID:[26667975](https://pubmed.ncbi.nlm.nih.gov/26667975/)
12. Loi S, Michiels S, Salgado R, Sirtaine N, Jose V, Fumagalli D, Kellokumpu-Lehtinen PL, Bono P, Kataja V, Desmedt C, Piccart MJ, Loibl S, Denkert C, et al. Tumor infiltrating lymphocytes are prognostic in triple negative breast cancer and predictive for trastuzumab benefit in early breast cancer: results from the FinHER trial. *Ann Oncol*. 2014; 25:1544–50.
<https://doi.org/10.1093/annonc/mdu112>
PMID:[24608200](https://pubmed.ncbi.nlm.nih.gov/24608200/)
13. Bianchini G, Balko JM, Mayer IA, Sanders ME, Gianni L. Triple-negative breast cancer: challenges and opportunities of a heterogeneous disease. *Nat Rev Clin Oncol*. 2016; 13:674–90.
<https://doi.org/10.1038/nrclinonc.2016.66>
PMID:[27184417](https://pubmed.ncbi.nlm.nih.gov/27184417/)
14. Hammerl D, Massink MP, Smid M, van Deurzen CH, Meijers-Heijboer HE, Waisfisz Q, Debets R, Martens JW. Clonality, antigen recognition, and suppression of CD8⁺ T cells differentially affect prognosis of breast cancer subtypes. *Clin Cancer Res*. 2020; 26:505–17.
<https://doi.org/10.1158/1078-0432.CCR-19-0285>
PMID:[31649042](https://pubmed.ncbi.nlm.nih.gov/31649042/)
15. Emens LA, Cruz C, Eder JP, Braithe F, Chung C, Tolaney SM, Kuter I, Nanda R, Cassier PA, Delord JP, Gordon MS, ElGaby E, Chang CW, et al. Long-term clinical outcomes and biomarker analyses of atezolizumab therapy for patients with metastatic triple-negative

- breast cancer: a phase 1 study. *JAMA Oncol.* 2019; 5:74–82.
<https://doi.org/10.1001/jamaoncol.2018.4224>
 PMID:[30242306](https://pubmed.ncbi.nlm.nih.gov/30242306/)
16. Topalian SL, Taube JM, Anders RA, Pardoll DM. Mechanism-driven biomarkers to guide immune checkpoint blockade in cancer therapy. *Nat Rev Cancer.* 2016; 16:275–87.
<https://doi.org/10.1038/nrc.2016.36>
 PMID:[27079802](https://pubmed.ncbi.nlm.nih.gov/27079802/)
 17. Li J, Byrne KT, Yan F, Yamazoe T, Chen Z, Baslan T, Richman LP, Lin JH, Sun YH, Rech AJ, Balli D, Hay CA, Sela Y, et al. Tumor cell-intrinsic factors underlie heterogeneity of immune cell infiltration and response to immunotherapy. *Immunity.* 2018; 49:178–93.e7.
<https://doi.org/10.1016/j.immuni.2018.06.006>
 PMID:[29958801](https://pubmed.ncbi.nlm.nih.gov/29958801/)
 18. Velcheti V, Schalper KA, Carvajal DE, Anagnostou VK, Syrigos KN, Sznol M, Herbst RS, Gettinger SN, Chen L, Rimm DL. Programmed death ligand-1 expression in non-small cell lung cancer. *Lab Invest.* 2014; 94:107–16.
<https://doi.org/10.1038/labinvest.2013.130>
 PMID:[24217091](https://pubmed.ncbi.nlm.nih.gov/24217091/)
 19. Lipson EJ, Vincent JG, Loyo M, Kagohara LT, Luber BS, Wang H, Xu H, Nayar SK, Wang TS, Sidransky D, Anders RA, Topalian SL, Taube JM. PD-L1 expression in the merkel cell carcinoma microenvironment: association with inflammation, merkel cell polyomavirus and overall survival. *Cancer Immunol Res.* 2013; 1:54–63.
<https://doi.org/10.1158/2326-6066.CIR-13-0034>
 PMID:[24416729](https://pubmed.ncbi.nlm.nih.gov/24416729/)
 20. Topalian SL, Hodi FS, Brahmer JR, Gettinger SN, Smith DC, McDermott DF, Powderly JD, Carvajal RD, Sosman JA, Atkins MB, Leming PD, Spigel DR, Antonia SJ, et al. Safety, activity, and immune correlates of anti-PD-1 antibody in cancer. *N Engl J Med.* 2012; 366:2443–54.
<https://doi.org/10.1056/NEJMoa1200690>
 PMID:[22658127](https://pubmed.ncbi.nlm.nih.gov/22658127/)
 21. Dirix LY, Takacs I, Jerusalem G, Nikolinakos P, Arkenau HT, Forero-Torres A, Boccia R, Lippman ME, Somer R, Smakal M, Emens LA, Hrinchenko B, Edenfield W, et al. Avelumab, an anti-PD-L1 antibody, in patients with locally advanced or metastatic breast cancer: a phase 1b JAVELIN solid tumor study. *Breast Cancer Res Treat.* 2018; 167:671–86.
<https://doi.org/10.1007/s10549-017-4537-5>
 PMID:[29063313](https://pubmed.ncbi.nlm.nih.gov/29063313/)
 22. Solinas C, Gombos A, Latifyan S, Piccart-Gebhart M, Kok M, Buisseret L. Targeting immune checkpoints in breast cancer: an update of early results. *ESMO Open.* 2017; 2:e000255.
<https://doi.org/10.1136/esmoopen-2017-000255>
 PMID:[29177095](https://pubmed.ncbi.nlm.nih.gov/29177095/)
 23. Ayers M, Lunceford J, Nebozhyn M, Murphy E, Loboda A, Kaufman DR, Albright A, Cheng JD, Kang SP, Shankaran V, Piha-Paul SA, Yearley J, Seiwert TY, et al. IFN- γ -related mRNA profile predicts clinical response to PD-1 blockade. *J Clin Invest.* 2017; 127:2930–40.
<https://doi.org/10.1172/JCI91190>
 PMID:[28650338](https://pubmed.ncbi.nlm.nih.gov/28650338/)
 24. Ueno Y, Ozaki S, Umakoshi A, Yano H, Choudhury ME, Abe N, Sumida Y, Kuwabara J, Uchida R, Islam A, Ogawa K, Ishimaru K, Yorozuya T, et al. Chloride intracellular channel protein 2 in cancer and non-cancer human tissues: relationship with tight junctions. *Tissue Barriers.* 2019; 7:1593775.
<https://doi.org/10.1080/21688370.2019.1593775>
 PMID:[30929599](https://pubmed.ncbi.nlm.nih.gov/30929599/)
 25. Yoshida N, Tsuzuki S, Karube K, Takahara T, Suguro M, Miyoshi H, Nishikori M, Shimoyama M, Tsukasaki K, Ohshima K, Seto M. STX11 functions as a novel tumor suppressor gene in peripheral t-cell lymphomas. *Cancer Sci.* 2015; 106:1455–62.
<https://doi.org/10.1111/cas.12742> PMID:[26176172](https://pubmed.ncbi.nlm.nih.gov/26176172/)
 26. Cheng WY, Ou Yang TH, Anastassiou D. Development of a prognostic model for breast cancer survival in an open challenge environment. *Sci Transl Med.* 2013; 5:181ra50.
<https://doi.org/10.1126/scitranslmed.3005974>
 PMID:[23596202](https://pubmed.ncbi.nlm.nih.gov/23596202/)
 27. Thomas ML. The leukocyte common antigen family. *Annu Rev Immunol.* 1989; 7:339–69.
<https://doi.org/10.1146/annurev.iy.07.040189.002011>
 PMID:[2523715](https://pubmed.ncbi.nlm.nih.gov/2523715/)
 28. Argenzio E, Moolenaar WH. Emerging biological roles of cl- intracellular channel proteins. *J Cell Sci.* 2016; 129:4165–74.
<https://doi.org/10.1242/jcs.189795> PMID:[27852828](https://pubmed.ncbi.nlm.nih.gov/27852828/)
 29. Gururaja Rao S, Patel NJ, Singh H. Intracellular chloride channels: novel biomarkers in diseases. *Front Physiol.* 2020; 11:96.
<https://doi.org/10.3389/fphys.2020.00096>
 PMID:[32116799](https://pubmed.ncbi.nlm.nih.gov/32116799/)
 30. Meng X, Wang G, Viero C, Wang Q, Mi W, Su XD, Wagenknecht T, Williams AJ, Liu Z, Yin CC. CLIC2-RyR1 interaction and structural characterization by cryo-electron microscopy. *J Mol Biol.* 2009; 387:320–34.
<https://doi.org/10.1016/j.jmb.2009.01.059>
 PMID:[19356589](https://pubmed.ncbi.nlm.nih.gov/19356589/)
 31. Choy CT, Wong CH, Chan SL. Embedding of genes using cancer gene expression data: biological relevance and potential application on biomarker discovery. *Front Genet.* 2019; 9:682.
<https://doi.org/10.3389/fgene.2018.00682>

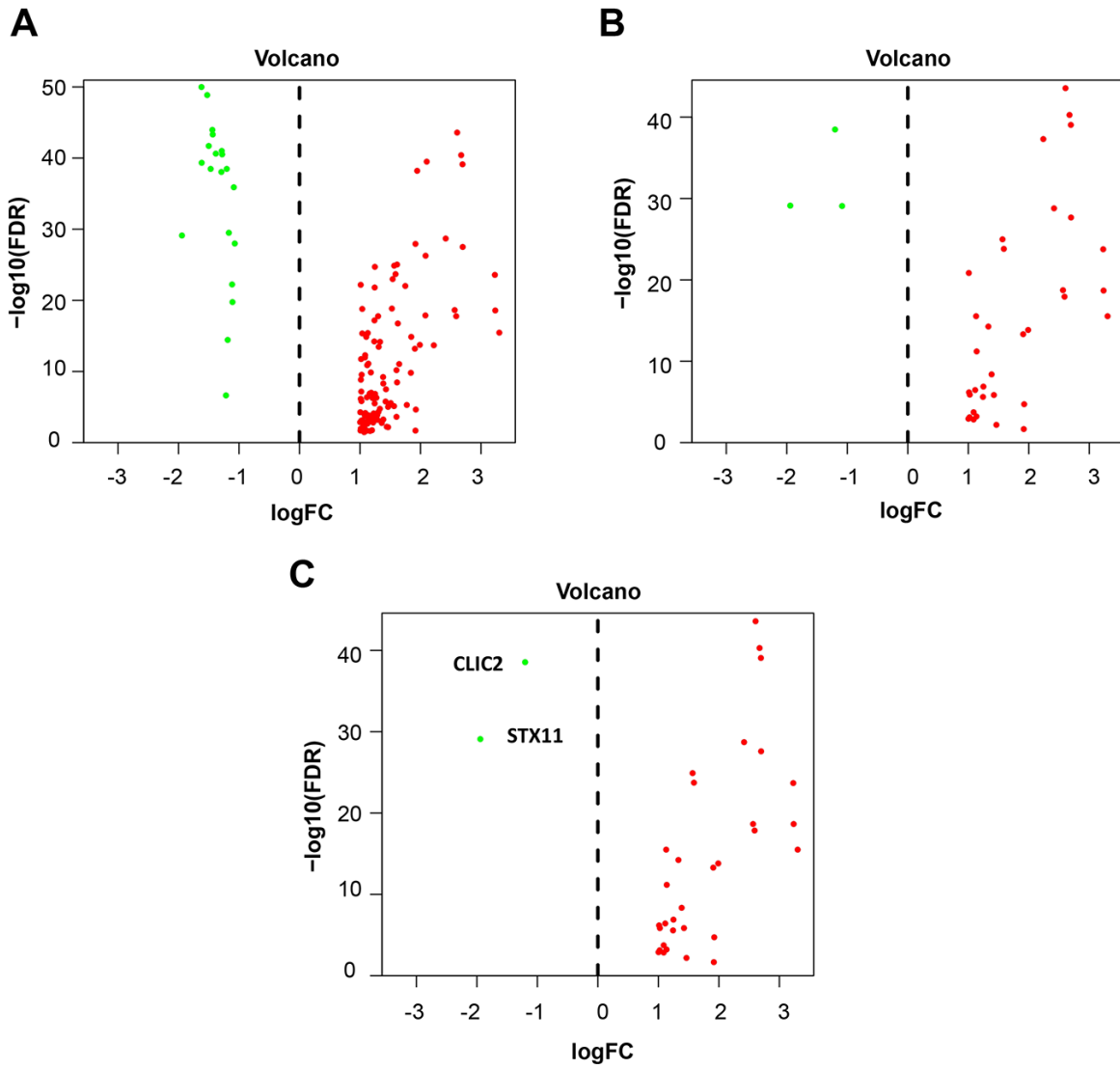
- PMID:[30662451](#)
32. Schreiber RD, Old LJ, Smyth MJ. Cancer immunoediting: integrating immunity's roles in cancer suppression and promotion. *Science*. 2011; 331:1565–70.
<https://doi.org/10.1126/science.1203486>
PMID:[21436444](#)
 33. Vesely MD, Kershaw MH, Schreiber RD, Smyth MJ. Natural innate and adaptive immunity to cancer. *Annu Rev Immunol*. 2011; 29:235–71.
<https://doi.org/10.1146/annurev-immunol-031210-101324> PMID:[21219185](#)
 34. Jiang T, Shi J, Dong Z, Hou L, Zhao C, Li X, Mao B, Zhu W, Guo X, Zhang H, He J, Chen X, Su C, et al. Genomic landscape and its correlations with tumor mutational burden, PD-L1 expression, and immune cells infiltration in Chinese lung squamous cell carcinoma. *J Hematol Oncol*. 2019; 12:75.
<https://doi.org/10.1186/s13045-019-0762-1>
PMID:[31299995](#)
 35. Paz-Ares L, Luft A, Vicente D, Tafreshi A, Gümüş M, Mazières J, Hermes B, Çay Şenler F, Csősz T, Fülöp A, Rodríguez-Cid J, Wilson J, Sugawara S, et al, and KEYNOTE-407 Investigators. Pembrolizumab plus chemotherapy for squamous non-small-cell lung cancer. *N Engl J Med*. 2018; 379:2040–51.
<https://doi.org/10.1056/NEJMoa1810865>
PMID:[30280635](#)
 36. R Development Core Team 3.0.1. A Language and Environment for Statistical Computing. *R Found Stat Comput* [Internet]. 2013; 2: <https://www.R-project.org>.
 37. Ritchie ME, Phipson B, Wu D, Hu Y, Law CW, Shi W, Smyth GK. Limma powers differential expression analyses for RNA-sequencing and microarray studies. *Nucleic Acids Res*. 2015; 43:e47.
<https://doi.org/10.1093/nar/gkv007>
PMID:[25605792](#)
 38. Zhang B, Horvath S. A general framework for weighted gene co-expression network analysis. *Stat Appl Genet Mol Biol*. 2005; 4:Article17.
<https://doi.org/10.2202/1544-6115.1128>
PMID:[16646834](#)
 39. Langfelder P, Horvath S. WGCNA: an R package for weighted correlation network analysis. *BMC Bioinformatics*. 2008; 9:559.
<https://doi.org/10.1186/1471-2105-9-559>
PMID:[19114008](#)
 40. Huang da W, Sherman BT, Lempicki RA. Systematic and integrative analysis of large gene lists using DAVID bioinformatics resources. *Nat Protoc*. 2009; 4:44–57.
<https://doi.org/10.1038/nprot.2008.211>
PMID:[19131956](#)
 41. Subramanian A, Tamayo P, Mootha VK, Mukherjee S, Ebert BL, Gillette MA, Paulovich A, Pomeroy SL, Golub TR, Lander ES, Mesirov JP. Gene set enrichment analysis: a knowledge-based approach for interpreting genome-wide expression profiles. *Proc Natl Acad Sci USA*. 2005; 102:15545–50.
<https://doi.org/10.1073/pnas.0506580102>
PMID:[16199517](#)
 42. Nagy Á, Lániczky A, Menyhárt O, Gyórfy B. Validation of miRNA prognostic power in hepatocellular carcinoma using expression data of independent datasets. *Sci Rep*. 2018; 8:9227.
<https://doi.org/10.1038/s41598-018-27521-y>
PMID:[29907753](#)
 43. Mizuno H, Kitada K, Nakai K, Sarai A. PrognoScan: a new database for meta-analysis of the prognostic value of genes. *BMC Med Genomics*. 2009; 2:18.
<https://doi.org/10.1186/1755-8794-2-18>
PMID:[19393097](#)
 44. Chen B, Lai J, Dai D, Chen R, Li X, Liao N. JAK1 as a prognostic marker and its correlation with immune infiltrates in breast cancer. *Aging (Albany NY)*. 2019; 11:11124–35.
<https://doi.org/10.18632/aging.102514>
PMID:[31790361](#)
 45. Gu Y, Li X, Bi Y, Zheng Y, Wang J, Li X, Huang Z, Chen L, Huang Y, Huang Y. CCL14 is a prognostic biomarker and correlates with immune infiltrates in hepatocellular carcinoma. *Aging (Albany NY)*. 2020; 12:784–807.
<https://doi.org/10.18632/aging.102656>
PMID:[31927532](#)
 46. Siemers NO, Holloway JL, Chang H, Chasalow SD, Ross-MacDonald PB, Voliva CF, Szustakowski JD. Genome-wide association analysis identifies genetic correlates of immune infiltrates in solid tumors. *PLoS One*. 2017; 12:e0179726.
<https://doi.org/10.1371/journal.pone.0179726>
PMID:[28749946](#)
 47. Mahmoud SM, Paish EC, Powe DG, Macmillan RD, Grainge MJ, Lee AH, Ellis IO, Green AR. Tumor-infiltrating CD8⁺ lymphocytes predict clinical outcome in breast cancer. *J Clin Oncol*. 2011; 29:1949–55.
<https://doi.org/10.1200/JCO.2010.30.5037>
PMID:[21483002](#)
 48. Liu Y, Patel L, Mills GB, Lu KH, Sood AK, Ding L, Kucherlapati R, Mardis ER, Levine DA, Shmulevich I, Broaddus RR, Zhang W. Clinical significance of CTNNB1 mutation and Wnt pathway activation in endometrioid endometrial carcinoma. *J Natl Cancer Inst*. 2014; 106:dju245.
<https://doi.org/10.1093/jnci/dju245>
PMID:[25214561](#)

SUPPLEMENTARY MATERIALS

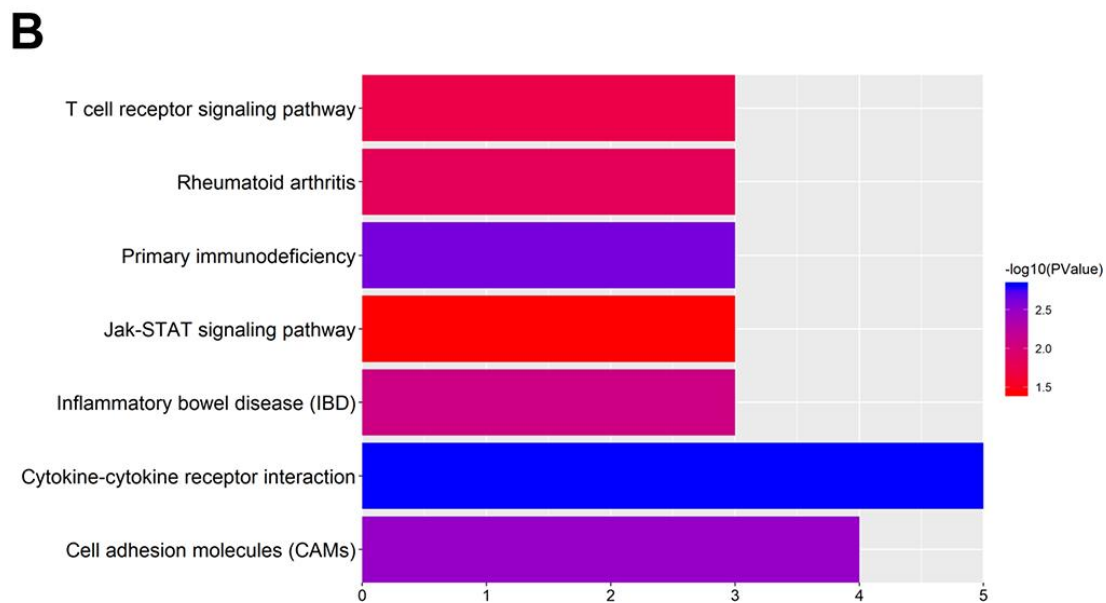
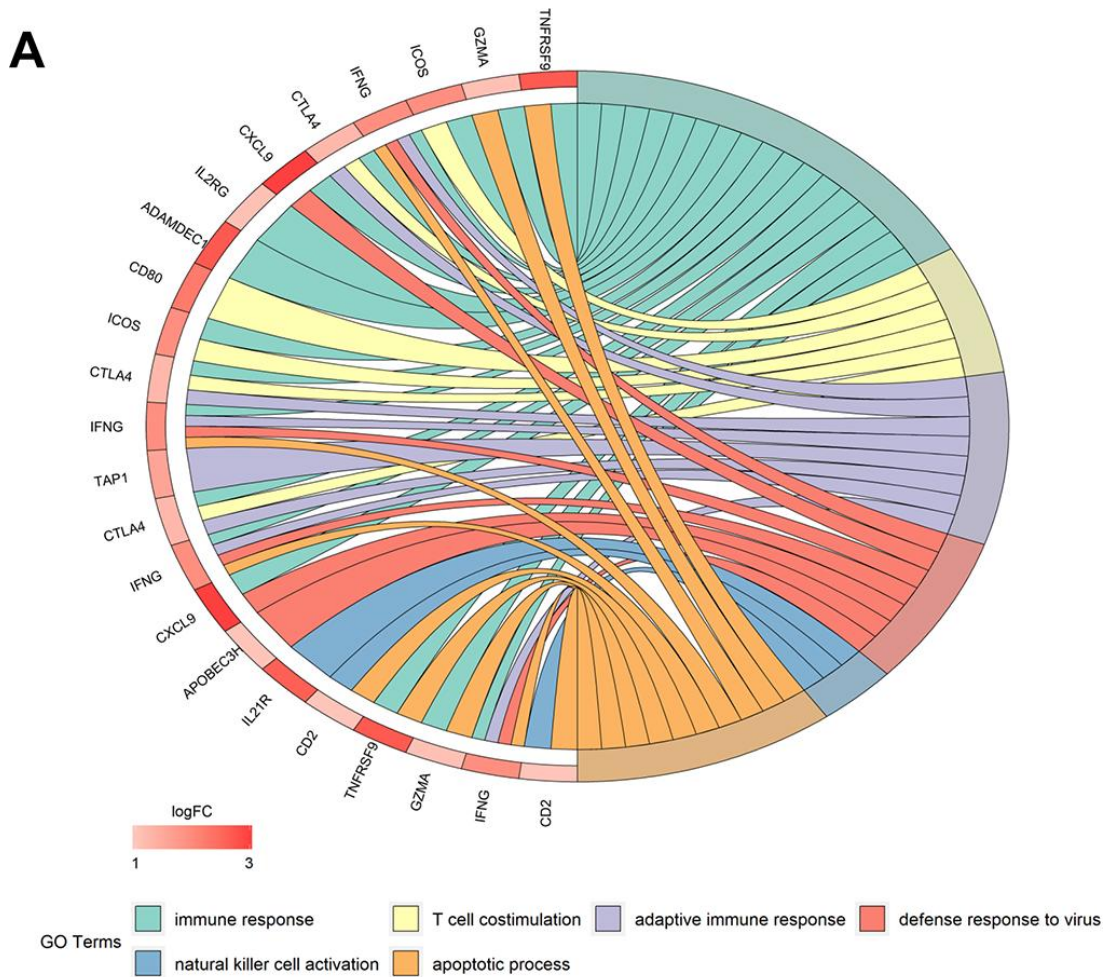
Supplementary Figures



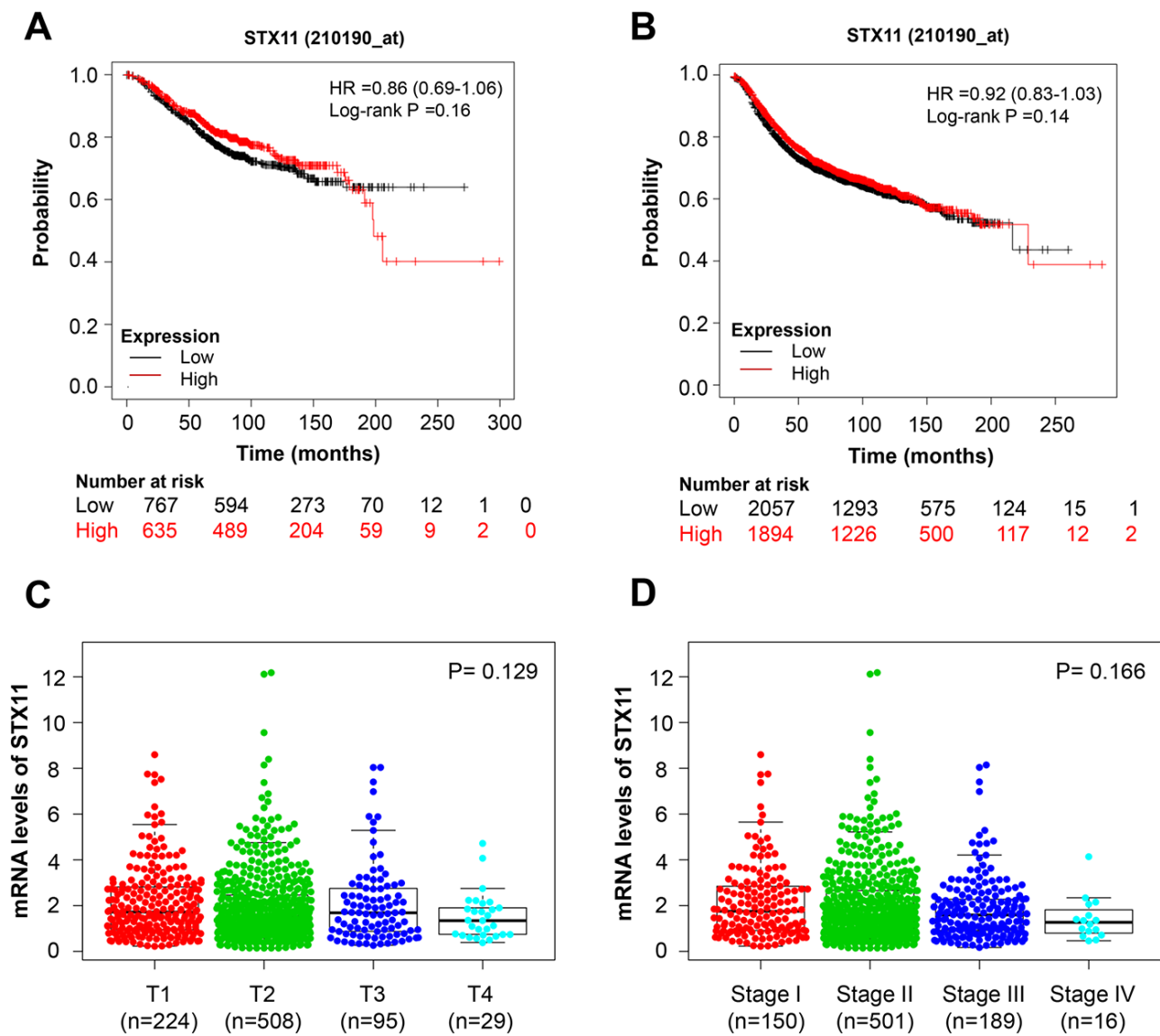
Supplementary Figure 1. DEGs between BC and normal tissue samples. (A) Volcano plot showing DEGs between BC (n = 1,053) and normal tissue (n = 111). Each bold dot denotes an individual gene with corrected $p < 0.05$ and $|\log_{2}(\text{fold-change (FC)})| > 1$. (B) Hierarchical clustering heatmap of DEGs. DEGs, differential expressed genes; FC, fold change.



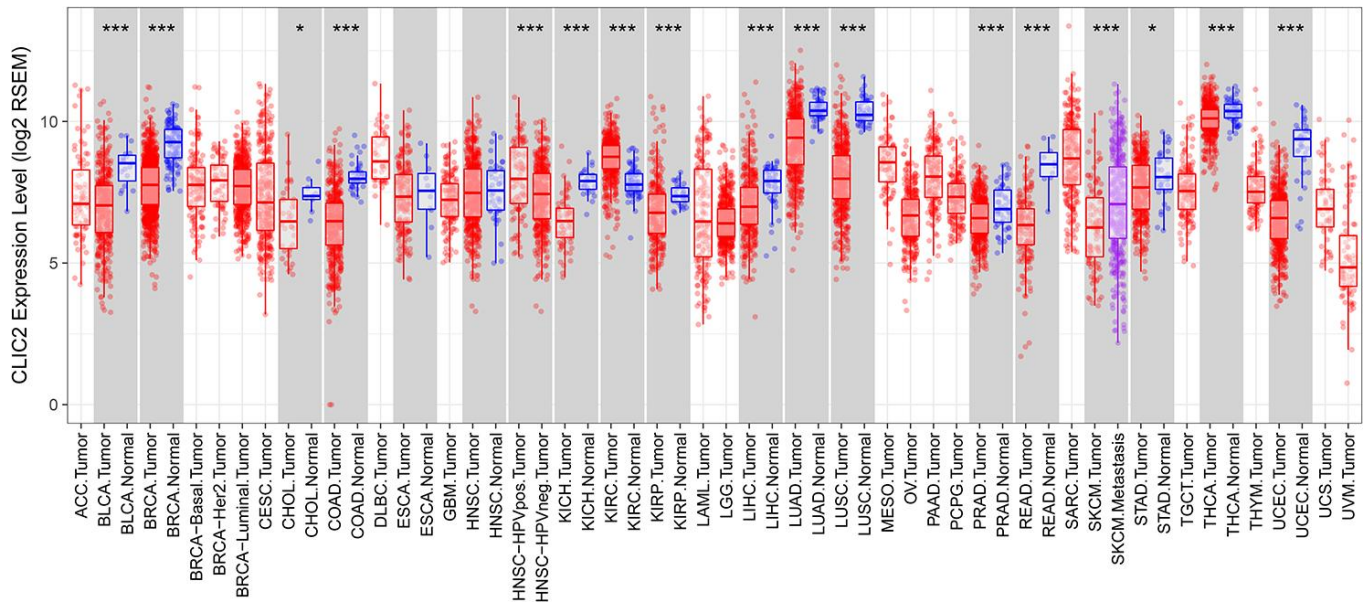
Supplementary Figure 2. Volcano plots of gene coexpression with PD-1 and PD-L1. (A) Volcano plot showing hub genes coexpression with PD-1. (B) Volcano plot showing hub genes coexpression with PD-L1. (C) Volcano plot showing hub genes coexpression with both PD-1 and PD-L1.



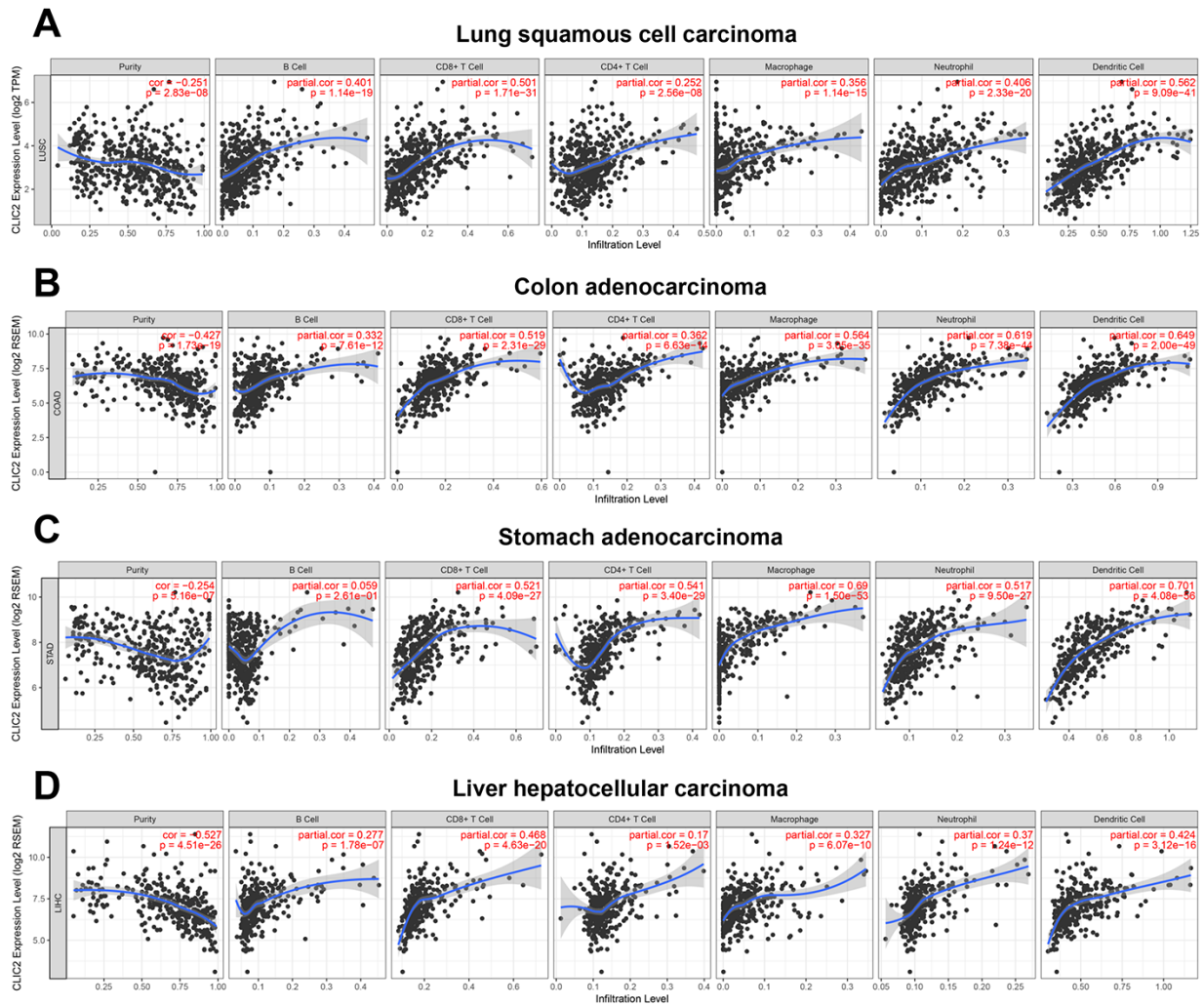
Supplementary Figure 3. GO term and KEGG pathway enrichment analysis for the hub gene cluster. (A) Major GO terms in hub gene clusters correlated to PD-L1 ($p < 0.05$). **(B)** Top-ranked KEGG pathways in hub gene clusters correlated to PD-L1 ($p < 0.05$). GO, gene ontology; KEGG, Kyoto Encyclopedia of Genes and Genomes.



Supplementary Figure 4. The relationship between STX11 and BC clinical performance. Kaplan-Meier estimation of OS (A) and RFS (B) of TCGA BC patients grouped by STX11 expression level. Expression levels of STX11 in BC with different tumor diameter (C) and in different stages (D). BC, breast cancer; OS, overall survival; PFS, progression-free survival.



Supplementary Figure 5. CLIC2 expression levels in different cancers. CLIC2 expression in different human cancers from TCGA database were shown by TIMER database. * $p < 0.05$, *** $p < 0.001$. TCGA, The Cancer Genome Atlas; TIMER, Tumor Immune Estimation Resource.



Supplementary Figure 6. CLIC2 highly expressed cancer types were accompanied by increased TILs. The TIMER database was used to assess the correlation between CLIC2 expression and six types of TILs enrichment cross four common cancers. TIMER analysis in (A) lung squamous cell carcinoma, (B) colon adenocarcinoma, (C) stomach adenocarcinoma, and (D) liver hepatocellular carcinoma. TILs, tumor infiltration lymphocytes; TIMER, Tumor Immune Estimation Resource.

Supplementary Tables

Supplementary Table 1. Screening PD-1/PD-L1 co-expressing genes by WGCNA method.

Description	Gene symbols
PD-L1 co-expressing Genes	CLIC2 GBP5 IFNG AL591468.1 LAG3 ADAMDEC1 CXCR2P1 SLAMF8 KCNJ10 CALHM6 USP30-AS1 IL21R EPSTI1 LINC02446 TAP1 IL2RG CXCL9 ICOS CD2 IL4I1 SNX20 STX11 PSMB9 CD80 GZMA OR2I1P PTPN7 CTLA4 ZBED2 TRAV12-3 CD300LF TNFRSF9 FGL2 TRAV25 TRAV26-1 TRAV2 APOBEC3H
PD-1 co-expressing genes	CLIC2 SIRPG PTPN7 IL2RG CXCR3 CORO1A CD2 CD3D CD27 TIGIT MAP4K1 IL21R CD6 MYO1G LTA SH2D1A TRBC2 CTLA4 TRBV20-1 GZMA CD7 SP140 CD5 SNX20 EOMES TRBV28 ITGAL AC004585.1 FUT7 GZMK TRAV12-3 TRBJ2-7 TRBV6-1 ICOS TRBV5-6 TRBV18 ZBED2 TRAV41 ZC3H12D TRBV12-4 TRBV11-2 FCRL3 CXCL9 TRBV6-6 CALHM6 FOXP3 RAB33A TRAV2 APOBEC3H TRAV26-1 TRBV4-2 GIMAP7 USP30-AS1 MIR155HG TRBV15 PLA2G2D TRAV39 LAG3 TRAV25 LTB LINC02446 GIMAP1 TRBV12-3 TRAV9-2 TRBV5-5 PNOC IFNG CD19 LINC01857 IGFLR1 HLA-DQB1 APBB1IP KCNJ10 TRAV26-2 ASB2 AC004687.1 STAP1 PSMB9 LIMD2 FCRLA LINC02273 SH2D2A TNFRSF9 SHISAL2A P2RX5 IL4I1 LINC01943 GIMAP5 LINC01215 CARMIL2 SLAMF8 TRAV6 PRDM8 SOWAHD IKZF3 MIAT CXCR2P1 RHOF MCOLN2 FCMR TRBV7-3 TRAT1 CASP17P PTGDS VSIR OR2I1P CFP SLC9A9 TCL1A CCR4 STX11 GBP5 EPSTI1 FAM129C PPP1R16B FLI1 ADAMDEC1 VPRESB3 GIMAP6 AL109914.1 TNFRSF4 TRDV1 AC108134.3 IFI30 RRN3P1 CLEC10A TNFRSF8 TAP1 AL591468.1 AIM2 GPR18

Supplementary Table 2. GO and KEGG analysis of PD-L1 co-expressing genes.

Term	Description	Count	P-value
GO:0006955	immune response	8	1.41757E-06
GO:0031295	T cell costimulation	3	0.005502265
GO:0002250	adaptive immune response	3	0.018757020
GO:0051607	defense response to virus	3	0.022989399
GO:0030101	natural killer cell activation	2	0.028215974
GO:0006915	apoptotic process	4	0.045793269
hsa04060	Cytokine-cytokine receptor interaction	5	0.001524288
hsa05340	Primary immunodeficiency	3	0.002391570
hsa04514	Cell adhesion molecules (CAMs)	4	0.003266245
hsa05321	Inflammatory bowel disease (IBD)	3	0.008275989
hsa05323	Rheumatoid arthritis	3	0.015247830
hsa04660	T cell receptor signaling pathway	3	0.019422333
hsa04630	JAK-STAT signaling pathway	3	0.038718075

Supplementary Table 3. Characteristics of patient subsets included in IHC analysis.

Parameters	Categories	No. of cases	Percentage (%)
Age, years (n=99)	20-30	1	1.01
	31-40	17	17.17
	41-50	45	45.45
	51-60	16	16.16
	61-95	20	20.20
Tumor Grade (n=98)	1	6	6.12
	2	71	72.45
	3	21	21.43
Tumor size, cm (n=83)	0.1-2.0	6	7.23
	2.1-5.0	68	81.93
	>5.0	9	10.84
Lymph node metastasis (n=99)	Present	24	24.24
	Absent	75	75.76
Distant Metastasis (n=99)	Present	0	0.00
	Absent	99	100.00
TNM Stages (n=99)	I	5	5.05
	II	72	72.73
	III	22	22.22
	IV	0	0.00
Molecular Subtype (n=98)	Luminal A	23	23.23
	Luminal B	44	44.44
	Her2 Positive	16	16.16
	TNBC	16	16.16
Relative quantification of TILs (n=99)	<20%	35	35.35
	20%-80%	43	43.43
	>80%	21	21.21